ResearchGate

See discussions, stats, and author profiles for this publication at: https://www.researchgate.net/publication/228045610

Greenish-yellow-, yellow-, and orange-light-emitting iridium(III) polypyridyl complexes with poly(ε-caprolactone)-bipyridine macroligands

ARTICLE *in* JOURNAL OF POLYMER SCIENCE PART A POLYMER CHEMISTRY · JULY 2005

Impact Factor: 3.11 · DOI: 10.1002/pola.20690

CITATIONS
43

READS
80

4 AUTHORS, INCLUDING:

Elisabeth Holder
Bergische Universität Wuppertal
58 PUBLICATIONS **1,979** CITATIONS

SEE PROFILE

Available from: Elisabeth Holder
Retrieved on: 24 January 2016

Greenish-Yellow-, Yellow-, and Orange-Light-Emitting Iridium(III) Polypyridyl Complexes with Poly(ϵ-caprolactone)–Bipyridine Macroligands

ELISABETH HOLDER,[1,2] VERONICA MARIN,[1,2] ALEXANDER ALEXEEV,[1,2] ULRICH S. SCHUBERT[1,2]

[1]Laboratory of Macromolecular Chemistry and Nanoscience, Eindhoven University of Technology, P.O. Box 513, 5600 MB Eindhoven, The Netherlands

[2]Dutch Polymer Institute, P.O. Box 902, 5600 AX Eindhoven, The Netherlands

Received 23 June 2004; accepted 6 December 2004
DOI: 10.1002/pola.20690
Published online in Wiley InterScience (www.interscience.wiley.com).

ABSTRACT: A set of novel greenish-yellow-, yellow-, and orange-light-emitting polymeric iridium(III) complexes were synthesized with the bridge-splitting method. The respective dimeric precursor complexes, $[Ir(ppy)_2\text{-}\mu\text{-}Cl]_2$ (ppy = 2-phenylpyridine) and $[Ir(ppy\text{–}CHO)_2\text{-}\mu\text{-}Cl]_2$ [ppy–CHO = 4-(2-pyridyl)benzaldehyde], were coordinated to 2,2′-bipyridine carrying poly(ϵ-caprolactone) tails. The resulting emissive polymers were characterized with one-dimensional (^{1}H) and two-dimensional (^{1}H–^{1}H correlation spectroscopy) nuclear magnetic resonance and infrared spectroscopy, gel permeation chromatography, and matrix-assisted laser desorption/ionization time-of-flight mass spectrometry, and the successful coordination of the iridium(III) centers to the 2,2′-bipyridine macroligand was revealed. The thermal behavior was studied with differential scanning calorimetry and correlated with atomic force microscopy. Furthermore, the quantitative coordination was verified by both the photophysical and electrochemical properties of the mononuclear iridium(III) compounds. The photoluminescence spectra showed strong emissions at 535 and 570 nm. The color shifts depended on the substituents of the cyclometallating ligands. Cyclic voltammetry gave oxidation potentials of 1.23 V and 1.46 V. Upon the excitation of the films at 365 nm, yellow light was observed, and this could allow potential applications in light-emitting devices. © 2005 Wiley Periodicals, Inc. J Polym Sci Part A: Polym Chem 43: 2765–2776, 2005

Keywords: atomic force microscopy (AFM); bipyridine macroligands; differential scanning calorimentry (DSC); light-emitting iridium(III) compounds; poly (ϵ-caprolactone); ring-opening polymerization; yellow-light-emitting films

INTRODUCTION

New metal-containing and emissive materials are finding applications in various research fields, such as labeling reagents for biological substrates and display materials.[1–9] Although d^6-transition metals such as ruthenium(II), osmium(II), and rhenium(II) polypyridine complexes have attracted considerable attraction, iridium(III) species are far less investigated, mainly because of synthetic problems in the past. Despite this fact, iridium(III) complexes are highly appealing because of their wide range of emission energies, long lifetimes, and high quantum yields.[10–12] The study of

Correspondence: U. S. Schubert (E-mail: u.s.schubert@tue.nl)

Journal of Polymer Science: Part A: Polymer Chemistry, Vol. 43, 2765–2776 (2005)
© 2005 Wiley Periodicals, Inc.

emissive and redox-active d^6-transition-metal complexes, such as those of iridium(III) and ruthenium(II), has been extended in recent years to applications in light-emitting devices and in light-emitting electrochemical cells.[13–27] For potential applications in such devices or in display technology, it is of importance to have phosphorescent emitters that are easily processed, do not aggregate or decay, and have high quantum yields and lifetimes of several microseconds. These requirements can be fulfilled if the emitted light results from metal-to-ligand charge-transfer (MLCT) processes. In this way, a variation of the ligand set may induce a change in the color of the emitted light. Despite these properties, the ligands of metal–ligand complexes can be used to introduce side chains, which can consist of various functionalities. 2,2′-Bipyridine (bpy) ligands are well known because of their remarkable chemistry as heterocyclic entities and because of their exceptional coordination chemistry.[28–30] The covalent linkage of the complex to a polymer leads to materials that reveal the advantage of preventing the aggregation of phosphors, as observed in polymer blends, while still maintaining the characteristics of the polymer backbone. This approach ensures processing features, known only for polymers such as spin coating and inkjet printing.[21,31–34] Furthermore, quick degradation on the electrode surface of the emitters might be prevented with this concept. A convenient way of obtaining such chelating diimine ligands equipped with polymer spacers is to perform a ring-opening polymerization (ROP) of ϵ-caprolactone.[35] With an appropriate catalyst and initiator, ROPs proceed in a controlled way, forming well-defined polymers with low polydispersity indices (PDIs) and adjustable molecular weights.[36] Using hydroxy-functionalized bpy's as coinitiators along with tin alkoxides allows the design of macroligands that prevent aggregation and degradation and have favorable processing properties for applications in device technology.

In this contribution, we describe the synthesis and characterization of a new set of iridium(III)-containing polymers based on a poly(ϵ-caprolactone)/2,2′-bipyridine (bpy–PCL) system. These new materials were synthesized with the coordination of known dimeric iridium(III) precursor complexes $[Ir(ppy)_2\text{-}\mu\text{-}Cl]_2$ (ppy = 2-phenylpyridine) and $[Ir(ppy\text{–}CHO)_2\text{-}\mu\text{-}Cl]_2$ [ppy–CHO = 4-(2-pyridyl)benzaldehyde] to bpy–PCL ligands.

EXPERIMENTAL

Instrumentation

One-dimensional (1D; ^1H) and two-dimensional [2D; ^1H–^1H correlation spectroscopy (COSY)] nuclear magnetic resonance (NMR) spectra were recorded on a Varian Gemini 300-MHz spectrometer at 298 K. Chemical shifts are reported in parts per million (δ) downfield from an internal standard, tetramethylsilane in CD_2Cl_2. Coupling constants (J values) are reported in hertz. Matrix-assisted laser desorption/ionization time-of-flight mass spectrometry (MALDI-TOF MS) was performed on a Voyager DE PRO biospectrometry workstation (Applied Biosystems) time-of-flight mass spectrometer reflector, with dithranol as a matrix. Infrared (IR) spectra were recorded on a PerkinElmer 1600 Fourier transform infrared spectrometer. Gel permeation chromatograms were measured on a Waters GPC system consisting of an isocratic pump, a solvent degasser, a column oven, a 2996 photodiode array detector, a 2414 refractive-index detector, a 717 Plus autosampler, and a Styragel HT 4 GPC column with a precolumn installed [dimethylformamide (DMF); 5 mM NH_4PF_6, 50 °C, 0.5 mL/min flow rate, poly(ethylene glycol) calibration]. Preparative size exclusion chromatography was performed on Biobeads S-X1 (CH_2Cl_2). UV spectra were recorded on a PerkinElmer Lambda-45 (1-cm cuvettes, CH_2Cl_2). Emission spectra were recorded on a PerkinElmer LS50B luminescence spectrometer (1-cm cuvettes, CH_2Cl_2). Electrochemical experiments were performed with an Autolab PGSTAT30 potentiostat. A standard three-electrode configuration was used, with platinum-bead working and auxiliary electrodes and a Ag/AgCl reference electrode. Ferrocene was added at the end of each experiment as an internal standard. The potentials are quoted versus the ferrocene/ferrocenium (Fe/Fe^+) couple. The solvent was CH_2Cl_2 (freshly distilled from CaH_2), containing 0.1 M $n\text{-}Bu_4PF_6$. The scanning rate was 100 mV/s. Elemental analyses were carried out on a EuroVector EuroEA3000 elemental analyzer for CHNS-O. Differential scanning calorimetry (DSC) investigations were performed on a PerkinElmer Pyris-1 DSC system at a heating rate of 40 K/min [melting temperature (T_m) and

glass-transition temperature (T_g)]. Atomic force microscopy (AFM) images were measured on a Solver47H (NT-MDT, Moscow, Russia) equipped with a heating stage allowing *in situ* heating of the samples up to 300 °C.

Materials and General Experimental Details

All manipulations were performed under an atmosphere of argon with the usual Schlenk techniques. All chemicals were reagent-grade and were used as received unless otherwise specified. Tin(II) 2-ethylhexanoate stannous octoate [$Sn(Oct)_2$], ppy, ppy–CHO, 2-ethoxyethanol, *N,N′*-carbonyl diimidazole, and ammonium hexafluorophosphate were purchased from Aldrich. ϵ-Caprolactone monomer was purchased from Fluka, and $IrCl_3 \cdot nH_2O$ was acquired from ABCR.

4-(3-Hydroxypropyl)-4′-methyl-2,2′-bipyridine (**1**) and the iridium(III) precursor complexes {tetrakis(2-phenylpyridine-C^2,N') (μ-dichloro)diiridium (**3**) and tetrakis[4-(2-pyridyl)benzaldehyde-C^2,N'] (μ-dichloro)diiridium (**4**)} were prepared according to literature methods.[2,37–39]

Poly(ϵ-caprolactone) (PCL)-Containing Bipyridine (2)

1 (initiator; 60 mg, 0.26 mmol) and ϵ-caprolactone (monomer; 1.04 g, 9.2 mmol) were stirred under an argon atmosphere until a temperature of 110 °C was reached. Then, a catalytic amount of stannous octoate was added, and the reaction mixture was stirred overnight. Precipitation from dichloromethane in methanol yielded 89% of **2** (calculated on the basis of the initiator).

IR: 3442 (OH), 2995, 2950 (CH aromatic), 1722 (C═O), 1370, 1295, 1240, 1170 (—CH_2—O—C═O—), 1047, 962, 733. ^{1}H NMR (CD_2Cl_2, δ, ppm): 1.83–1.03 (m, H, f′, e′, and g′), 2.04–1.87 (m, 2H, b′), 2.33–2.05 (m, H, d′), 2.36 (s, 2H, a), 2.77–2.64 (m, 2H, a′), 3.58–3.44 (m, 2H, H′), 4.29–3.44 (m, H, c′ and h′), 7.07 (s, 2H, 5,5′), 8.21 (d, 2H, J = 5.50 Hz, 3,3′), 8.43 (dd, 2H, J = 4.94, 10.98 Hz, 6,6′). Ultraviolet–visible (UV–vis; CH_2Cl_2): [λ_{max} (nm); $\epsilon = E/l*c$(L mol^{-1} cm^{-1})] = 282 (9.9×10^3), 242 (7.6×10^3). MALDI-TOF MS (dithranol): (M_n) = 3470 g × mol^{-1}, (M_w) = 4340 g × mol^{-1}, PDI = 1.25. GPC (DMF): M_n = 4120 g × mol^{-1}, M_w = 5800 g × mol^{-1}, PDI = 1.40. T_m: 56.2 °C. T_g: −52.8 °C.

Tetrakis(2-phenylpyridine-C^2,N′) (μ-Dichloro)diiridium {[Ir(ppy)$_2$Cl]$_2$ or 3}

Iridium trichloride hydrate (0.388 g, 26 mmol) was combined with ppy (0.76 g, 64 mmol), dissolved in a mixture of 2-ethoxyethanol (30 mL) and water (10 mL), and refluxed for 24 h. The solution was cooled to room temperature, and the yellow precipitate was collected on a glass filter frit. The precipitate was washed with ethanol (60 mL) and acetone (60 mL) and then was dissolved in dichloromethane (75 mL) and filtered. Toluene (25 mL) and hexanes (10 mL) were added to the filtrate, which was then reduced in volume by evaporation to 50 mL and cooled to give crystals of **3** in a 72% yield (0.428 g).

IR: 3058 (C═C), 1605, 1581, 1476, 1414, (C═C and C═N), 1305, 1267, 1224, 1159, 1061, 1029, 753, 734, 727, 669. ^{1}H NMR (CD_2Cl_2, δ): 5.86 (d, J = 7.91 Hz, 2H, $H^{D'}$), 6.59 (t, J = 7.03 Hz, 2H, $H^{C'}$), 6.74–6.97 (m, 4H, H^C and $H^{B'}$), 7.54 (d, 2H, J = 7.03 Hz, $H^{A'}$), 7.72–7.86 (m, 2H, H^B), 7.92 (d, 2H, J = 7.91 Hz, H^A), 9.24 (d, 2H, J = 6.15 Hz, H^D). UV–vis (CH_2Cl_2): λ_{max} [nm; ϵ (L mol^{-1} cm^{-1})] = 263 (6.5×10^4), 300 (2.8×10^4), 370 (7.4×10^3), 440 (3.8×10^3). MALDI-TOF MS (dithranol): m/z = 1040.32 [$Ir_2C_{44}H_{32}N_4C1_2$]—Cl. Elem. Anal. Calcd. for $Ir_2C_{44}H_{32}N_4C1_2$ (1075.82): C, 49.29%; H, 3.01%; N, 5.23%. Found: C, 49.58%; H, 3.16%; N, 5.09%.

Tetrakis[4-(2-pyridyl)benzaldehyde-C^2,N′] (μ-Dichloro)diiridium {[Ir(ppy–CHO)$_2$Cl]$_2$ or 4}

Iridium trichloride trihydrate (388 mg, 1.1 mmol) was combined with ppy–CHO (403 mg, 2.2 mmol), dissolved in a mixture of 2-ethoxyethanol (30 mL) and water (10 mL), and refluxed for 24 h (the solution was purged with argon and stirred in the dark). The solution was cooled to room temperature, and the orange precipitate was collected on a glass filter frit. The precipitate was washed with ethanol (60 mL) and acetone (60 mL) and then was dissolved in dichloromethane (75 mL) and filtered over a Celite pad. After partial evaporation, *n*-hexane (50 mL) was added to the solution to grow orange crystals of **4** in a 53% yield (623 mg).

IR: 2828 (C═C), 1682 (aldehydic C═O), 1605, 1562, 1475 (C═C and C═N), 1367 (aldehydic C—H), 1183, 1052, 887, 753, 744, 672. ^{1}H NMR (CD_2Cl_2, δ): 6.30 (s, 2H, $H^{I'}$), 6.99 (dt, J = 1.09, 6.04 Hz, 2H, H^G), 7.29 (d, 2H, J = 8.24 Hz, $H^{F'}$), 7.71 (d, 2H, J = 8.24 Hz, $H^{E'}$), 7.95 (dt, 2H, J = 1.09, 7.7 Hz, H^F), 8.09 (d, 2H, J = 7.7 Hz, H^E), 9.25 (d, 2H, J = 6.04 Hz, H^I), 9.49 (s, 2H, CHO).

UV–vis (CH_2Cl_2): λ_{max} [nm; ϵ (L mol^{-1} cm^{-1})] = 263 (6.5×10^4), 283 (7.5×10^4), 310 (6.4×10^4), 370 (9.4×10^3), 440 (5.4×10^3), 475 (5.0×10^3). MALDI-TOF MS (dithranol): *m/z* = 1149.17 [$Ir_2C_{48}H_{32}N_4O_4C1_2$]—Cl, 594.21 [$IrC_{24}H_{18}N_2O_2C1$], 557.24 [$IrC_{24}H_{18}N_2O_2$]. ELEM. ANAL. Calcd. for $Ir_2C_{48}H_{32}N_4O_4C1_2$ (1184.15) C, 48.69%; H, 2.72%; N, 4.73%. Found: C, 48.49%; H, 3.02%; N, 4.37%.

Iridium(III) Macroligand Complex (5)

A solution of **3** (42 mg, 0.038 mmol) in methanol (10 mL) was added to a suspension of macroligand **2** (110 mg, 0.038 mmol) in dichloromethane (8 mL). Heated under reflux conditions for 12 h, the starting suspension became a clear yellow solution. After the solution cooled to room temperature, a saturated solution of [NH_4][PF_6] in methanol (2 mL) was added, and stirring was continued for another 12 h. Partial evaporation of the solvents under reduced pressure afforded a yellow polymer. To remove excessive [NH_4][PF_6], the complex was redissolved in dichloromethane and extracted (3 × 20 mL of H_2O); this was followed by purification by preparative size exclusion chromatography (Biobeads S-X1, CD_2Cl_2) and precipitation in *n*-hexane. The yield was 123 mg (86%) of **5**.

IR: 3442 (OH), 2944, 2865 (CH aromatic), 1722 (C═O), 1370, 1293, 1239, 1171 (—CH_2—O—C═O—), 1045, 962, 841 (PF_6), 731. ^{1}H NMR (CD_2Cl_2, δ, ppm): 1.29–2.04 (m, $H^{f'}$, $H^{e'}$, and $H^{g'}$), 2.07–2.62 (m, $H^{b'}$ and $H^{d'}$), 2.66 (s, 3H, H^a), 2.92–3.06 (m, 2H, $H^{a'}$), 3.60–3.72 (m, 2H, $H^{H'}$), 3.78–4.53 (m, $H^{c'}$ and $H^{h'}$), 6.37–6.20 (m, 2H, ppy), 7.13–6.83 (m, 6H, 5,5′-bpy, ppy), 7.29–7.16 (m, 2H, ppy), 7.58–7.44 (m, 2H, ppy), 8.04–7.63 (m, 8H, 6,6′-bpy, ppy), 8.43–8.25 (m, 2H, 3,3′-bpy). UV–vis (CH_2Cl_2): λ_{max} [nm; ϵ (L mol^{-1} cm^{-1})] = 260 (1.7×10^5), 305 (7.9×10^4), 370 (2.2×10^4), 420 (1.1×10^4). MALDI-TOF MS (dithranol): M_n = 3950 g × mol^{-1}, M_w = 4180 g × mol^{-1}, PDI = 1.06. GPC (DMF): M_n = 5300 g × mol^{-1}, M_w = 6700 g × mol^{-1}, PDI = 1.27. T_m: 58.0 °C. T_g: −59.2 °C.

Iridium(III) Macroligand Complex (6)

A solution of **4** (42 mg, 0.038 mmol) in methanol (10 mL) was added to a suspension of macroligand **2** (110 mg, 0.038 mmol) in dichloromethane (8 mL). Heated under reflux conditions for 12 h, the starting suspension became a clear yellow solution. After the solution cooled to room temperature, a saturated solution of [NH_4][PF_6] in methanol (2 mL) was added, and stirring was continued for another 12 h. Partial evaporation of the solvents under reduced pressure afforded a yellow polymer. To remove excessive [NH_4][PF_6], the complex was redissolved in dichloromethane and extracted (3 × 20 mL of H_2O); this was followed by purification by preparative size exclusion chromatography (Biobeads S-X1, CD_2Cl_2) and precipitation in *n*-hexane. The yield was 134 mg (93%) of **6**.

IR: 3442 (OH), 2945, 2865 (CH aromatic), 1722 (C═O, CHO), 1365 (aldehydic C—H), 1293, 1238, 1170 (—CH_2—O—C═O—), 1044, 961, 840 (PF_6), 798, 731. ^{1}H NMR (CD_2Cl_2, δ, ppm): 1.03–1.84 (m, $H^{f'}$, $H^{e'}$ and $H^{g'}$), 1.90–2.06 (m, 2H, $H^{b'}$), 2.07–2.35 (m, $H^{d'}$), 2.53 (s, 3H, H^a), 2.85 (t, 2H, J = 7.26 Hz, $H^{a'}$), 3.50 (t, 2H, J = 6.45 Hz, $H^{H'}$), 3.63–4.27 (m, $H^{c'}$ and $H^{h'}$), 6.65 (d, 2H, J = 4.03 Hz, $H^{I'}$), 7.10 (t, 2H, J = 7.26 Hz, H^G), 7.18 (t, 2H, J = 5.64 Hz, H^5 and $H^{5'}$), 7.47 (d, 2H, J = 8.06 Hz, $H^{F'}$), 7.54 (t, 2H, J = 6.45 Hz, H^I), 7.72 (dd, 2H, J = 5.64, 12.09 Hz, H^6 and $H^{6'}$), 7.79–7.92 (m, 4H, H^F and $H^{E'}$), 8.03 (d, 2H, J = 8.06 Hz, H^E), 8.34 (s, 2H, H^3 and $H^{3'}$) 9.64 (s, 2H, CHO). UV–vis (CH_2Cl_2): λ_{max} [nm; ϵ (L mol^{-1} cm^{-1})] = 270 (1.5×10^5), 297 (1.2×10^5), 370 (2.1×10^4), 430 (1.2×10^4). MALDI-TOF MS (dithranol): M_n = 3830 g × mol^{-1}, M_w = 4050 g × mol^{-1}, PDI = 1.06. GPC (DMF): M_n = 7280 g × mol^{-1}, M_w = 9400 g × mol^{-1}, PDI = 1.29. T_m: 58.6 °C. T_g: −49.1 °C.

Sample Preparation for AFM Measurements

To obtain single crystals of polymer **6**, a piece of mica was immersed in a hot acetonitrile solution (temperature = 70 °C, concentration = 10^{-5} mol/L) of **6** and dried at room temperature. The sample was exposed to increasing temperature with the heating stage of the AFM instrument. The changes in the sample were visualized at 20, 41, 47, 53, 55, and 57 °C.

RESULTS AND DISCUSSION

Synthesis and Characterization

A hydroxy-modified bipyridine was obtained through the reaction of monolithiated 4,4′-dimethyl-2,2′-bipyridine with 2-bromoethoxy-*tert*-butyldimethylsilane, followed by the cleavage of the Si—O bond in a strong acidic medium; this led to a 47% yield of **1**.[21] Subsequently, a controlled ROP of ϵ-caprolactone was performed in bulk with

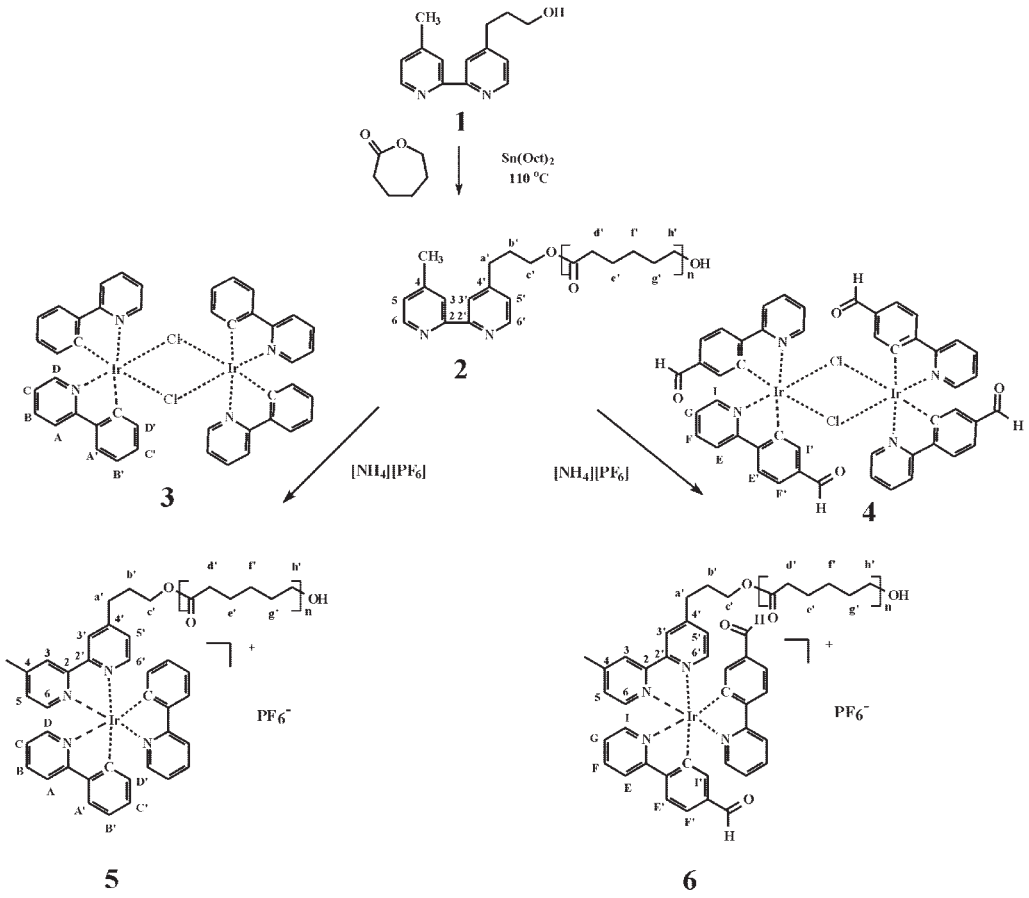

Scheme 1. Schematic presentation of the synthesis of macroligand complexes **5** and **6** (n = 30).

hydroxy-functionalized bpy **1** as the initiator and with $Sn(Oct)_2$ as the catalyst (Scheme 1).[35,36] Precipitation from dichloromethane in methanol yielded 89% of macroligand **2**, which was soluble in organic solvents of medium polarity. Campagna et al.[39] introduced a general and straightforward synthetic strategy for the synthesis of small-molecule mixed-ligand orthometallated iridium(III) complexes with high yields and high purity. The complexation of the orthometallated dimeric complexes $[Ir(N\hat{}C)_2Cl]_2$ [where N^C is 2-phenylpyridine$^-$ (ppy$^-$; **3**) or 4-(2-pyridyl)-benzaldehyde$^-$ (ppy–CHO$^-$; 4)] yielded the monomeric mixed-macroligand iridium(III) complexes **5** and **6** {$[Ir\text{-}(N\hat{}C_2(bpy–PCL)]^+$} via a bridge-splitting reaction exploiting chelating polymeric bipyridine **2**. The reaction was carried out in a refluxing dichloromethane/methanol mixture (1/10 v/v). Macroligand complexes **5** and **6** were precipitated with a saturated methanolic $[NH_4][PF_6]$ solution (exchange of counterions). The excess of ammonium hexafluorophosphate was extracted with water. Purification by preparative size exclusion chromatography, followed by precipitation in n-hexane, afforded **5** and **6** in 86 and 93% yields, respectively. The yellow monocationic complex **5** and the yellow-orange monocationic complex **6** were soluble in organic solvents of medium-to-high polarity.

In the ^{1}H NMR spectrum of macroligand **2**,[40] the aromatic signals remained unshifted in comparison with those of parent bipyridine **1**, and this proved the successful incorporation of the bipyridine ligand into the PCL backbone. The orthometallated iridium(III) precursor structures **3** and **4** were investigated with 2D ^{1}H–^{1}H COSY [Fig. 1(A)]; the cross peaks corresponding to the two- and three-bond correlations (H—C—H and H—C—C—H) allowed an identification of all the signals.

The ^{1}H NMR spectra proved the complete coordination of bipyridine macroligand **2** to iridium

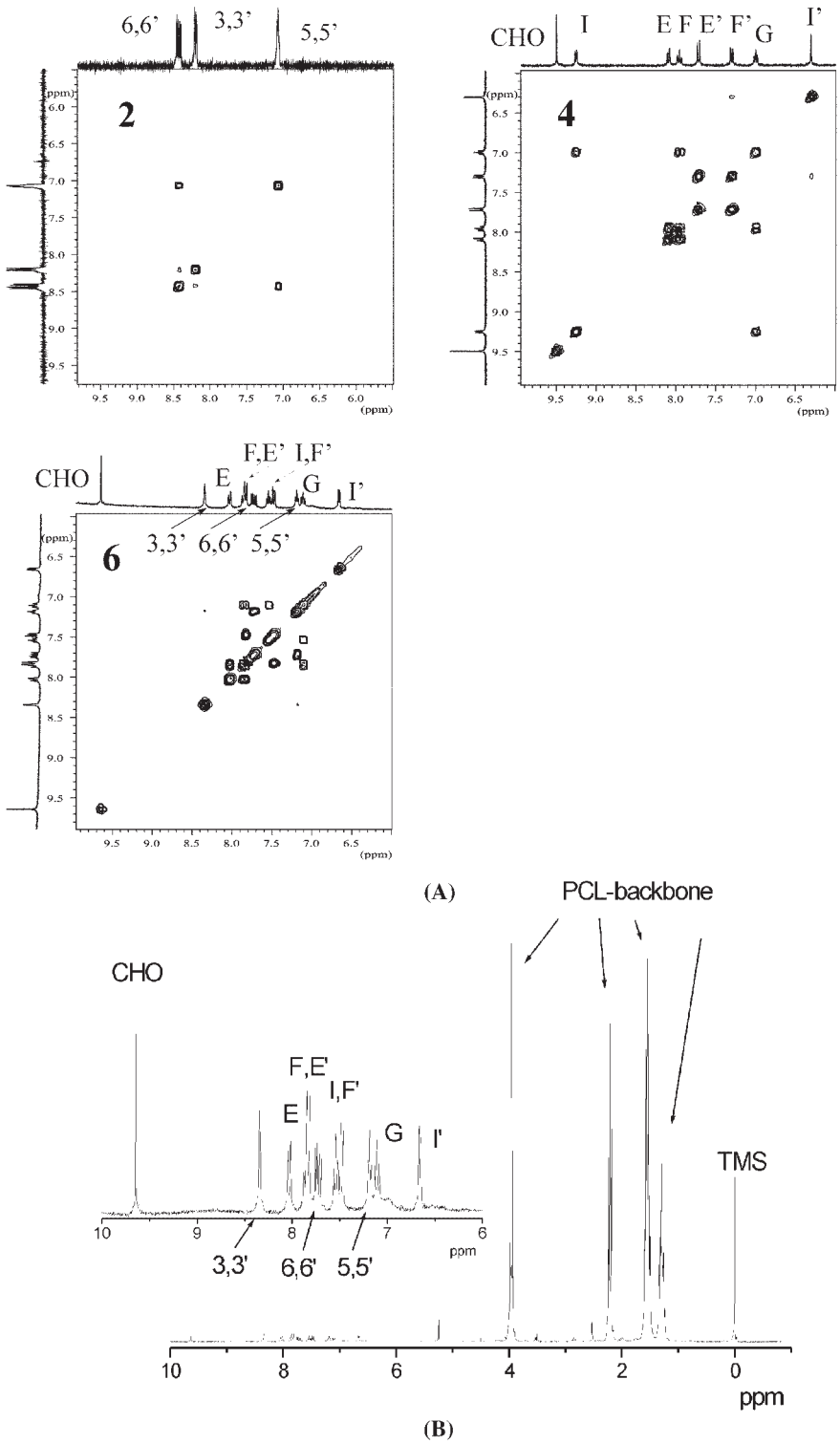

Figure 1. (A) ^{1}H–^{1}H COSY spectra of **2**, **4**, and **6** in CD_2Cl_2 (expansions of the aromatic regions of **2**, **4**, and **6** are displayed) and (B) complete 1D NMR spectrum of **6** recorded in CD_2Cl_2 (the full spectral range is displayed, showing the characteristic resonances of the PCL backbone; the inset represents the aromatic region with the expected resonances for one coordinated functionalized bpy ligand and two ppy–CHO ligands).

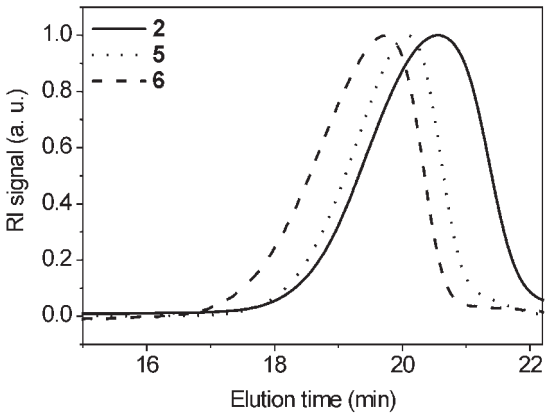

Figure 2. GPC elution chromatograms for macroligand **2** and complexes **5** and **6**.

precursor complexes **3** and **4**, the integration of the aromatic protons being evidence of the presence of one bpy–PCL macroligand and two ppy (**5**) and two benzaldehyde pyridine (**6**) ligands, respectively. Figure 1(B) exemplifies the 1D NMR spectra, displaying the full spectral range of **6**. The inset shows an expansion of the aromatic region of **6**. One example of the successful complexation of the bipyridine macroligand with the benzaldehyde pyridine is presented in Figure 1(A) (^{1}H–^{1}H COSY spectra of macroligand **2**, iridium(III) precursor **4**, and macroligand complex **6**).[41] Only the aromatic region is displayed for all three compounds because there is no significant effect on the aliphatic PCL backbone resonances upon the complexation of the bipyridine macroligand. For **6**, a large upfield shift was detected for the H^6 and $H^{6'}$ bipyridine protons in comparison with those of free ligand **2**, whereas for the $H^{3,3'}$ and $H^{5,5'}$ bipyridine resonances, a small downfield shift was visible. Moreover, there was a clear change in the H^I protons from the pyridine ring toward lower frequencies.

The observed IR vibration bands (monitored from 4000 to 650 cm^{-1}) for precursor complexes **3** and **4** were dominated by the respective cyclometallating ligands ppy and ppy–CHO. Comparing precursor complexes **3** and **4** showed significant differences: additional vibration bands occurred because of the aldehyde functionality of **4**. These additional strong bands were observed at 1682 (C═O aldehydic stretching vibrations) and 1367 cm^{-1} (C—H aldehydic bending vibrations). The IR vibration properties of macroligand complexes **5** and **6** were dominated by the absorption of the PCL backbone; intense bands appeared at 3442 (OH stretching vibration), 1722 (C═O stretching vibration of the esters), and 1170 cm^{-1} (—CH_2—O—C═O—; assigned to C—O stretching vibrations of the esters). For complex **6**, the significant CHO stretching vibration (for compound **4** at 1682 cm^{-1}) overlapped the PCL —C═O— stretching vibration, with a maximum absorbance at 1722 cm^{-1}, and was recognizable as a distinct shoulder toward higher frequencies. Moreover, the characteristic band of the hexafluorophosphate counterion at 840 cm^{-1} was visible for polymeric complexes **5** and **6**.

The purity and stability of polymer **2** and macroligand complexes **5** and **6** were investigated by GPC with an optimized eluent (Fig. 2).[42] For all elution runs, monomodal distributions were observed. No fragmentation of the metal-to-ligand bonds was detected during the elution on the chromatographic column. The slight shift of the elution bands might be an effect of the different hydrodynamic volumes of the investigated materials.

Polymers **2**, **5**, and **6** were additionally characterized by MALDI-TOF MS. Figure 3 shows the MALDI mass spectra of macroligand **2** and corresponding complexes **5** and **6**, respectively. The molecular weight distributions were shifted toward higher molecular weights upon the complexation of polymer **2** with the ppy (**3**) and ppy–CHO (**4**) precursor complexes. For both macroligand complexes, only one distribution was observed in the MALDI spectrum. Also, no dissociation of the metal-to-ligand bonds occurred during the laser desorption/ionization process. Therefore, MALDI-TOF MS presents a valuable

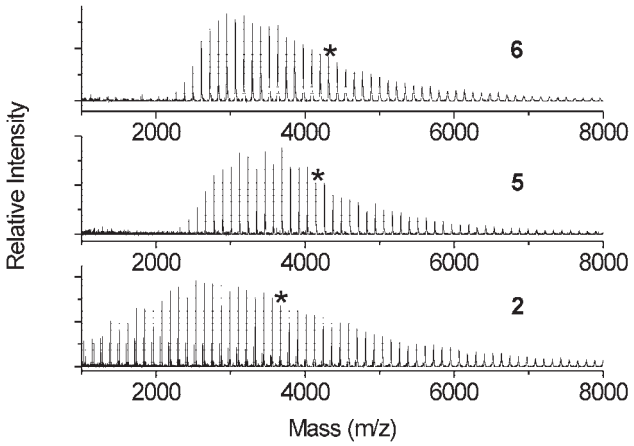

Figure 3. MALDI-TOF MS spectra for bpy–PCL **2** and PCL-based polymers **5** and **6**. The peaks marked with asterisks correspond to $n = 30$. The second distribution visible in the recorded MALDI-TOF MS spectrum for compound **2** can be assigned to Na^+ adducts.

Table 1. MALDI TOF-MS and GPC Characterization Data of **2, 5,** and **6**

	MALDI TOF-MS			GPC			NMR
Compound	M_n ($g \times mol^{-1}$)	M_w ($g \times mol^{-1}$)	PDI	M_n ($g \times mol^{-1}$)	M_w ($g \times mol^{-1}$)	PDI	M_n ($g \times mol^{-1}$)
2	3470	4340	1.25	4120	5800	1.40	5540
5	3950	4180	1.06	5300	6700	1.27	5806
6	3830	4050	1.06	7280	9400	1.29	5750

supplementary tool for the characterization and identification of polypyridyl-based polymer **2** and mononuclear iridium(III) compounds **5** and **6**. Table 1 summarizes molecular weight parameters obtained by NMR spectroscopy, GPC, and MALDI-TOF MS for **2**, **5**, and **6**.

DSC and AFM

For characterizing the apparent phase-transition temperatures (for glass-transition, melting, and crystallization processes) of new polymeric materials, DSC is a convenient method. A thermal analysis was performed on **2** (T_m = 56.2 °C, ΔH = 77.0 J/g, T_g = −52.8 °C, Δc_p = 0.15 J/g °C) and macroligand complexes **5** (T_m = 58.0 °C, ΔH = 65.5 J/g, T_g = −59.2 °C, Δc_p = 0.18 J/g °C) and **6** (T_m = 58.6 °C, ΔH = 71.9 J/g, T_g = −49.1 °C, Δc_p = 0.23 J/g °C), and it revealed no significant influence of the incorporation of the metal complex centers into the macroligand (Fig. 4). For **6**, the phase transition from solid to liquid could be visualized by AFM, as presented in Figure 5. For this experiment, single crystals were grown on a mica substrate via the dip coating of the substrate into a hot diluted acetonitrile solution of **6**.[43,44] The AFM images of a single crystal of **6** are depicted in Figure 5 and characterize the melting process of **6**. The height of the intact single crystal of **6** was determined by AFM to be 7 nm (Fig. 5 at 20 °C). Upon the gradual heating of the substrate, the intact single crystal (Fig. 5 at 20 °C) started to melt slowly with increasing temperature. The melting process is shown for five different temperatures. The image for 57 °C shows the completed phase transition of the molten crystal of **6**. The T_m value obtained by AFM correlates with the DSC results within the experimental error.

Photophysical and Electrochemical Properties

Figure 6 shows the UV–vis characterization data of complexes **3** and **4** and the corresponding polymers **5** and **6** in dichloromethane solutions (see also Table 2). For complexes **3** and **5**, the strong absorption band at about 270 nm was attributed to the ligand-centered $\pi \rightarrow {}^*\pi$ transitions on ppy^- and bpy. For complexes **4** and **6**, the strong absorption bands at about 270 and 300 nm were attributed to the ligand-centered $\pi \rightarrow {}^*\pi$ transitions on bpy and on cyclometallating ppy–CHO^-. The broad absorption bands at a lower energy (ca. 370 nm) were due to typical spin-allowed ^{1}MLCT transitions [$d\pi$(Ir)$\rightarrow {}^*\pi$ bpy and ppy–CHO^- transitions]. For **6**, the shoulder tailing to 440 nm was assigned to spin-forbidden ^{3}MLCT transitions [$d\pi$(Ir)$\rightarrow {}^*\pi$ bpy and ppy–CHO^- transitions].[2,30,39] In both cases, dimeric precursor complexes **3** and **4** revealed weak absorption bands in lower energy regions than mononuclear iridium(III) compounds **5** and **6**. Figure 7 displays the emission properties of complexes **5** and **6** both in solutions and as films. The excitation of iridium macromolecules **5** and **6** at 370 nm revealed broad emission bands for solutions basically derived from ^{3}IL $\pi \rightarrow {}^*\pi$ transitions on the ppy^- and ppy–CHO^- excited states. Moreover, there might also be some ^{3}MLCT [$d\pi$(Ir)$\rightarrow {}^*\pi$ ppy^- and ppy–CHO^-] excited states involved.[2,10] Excita-

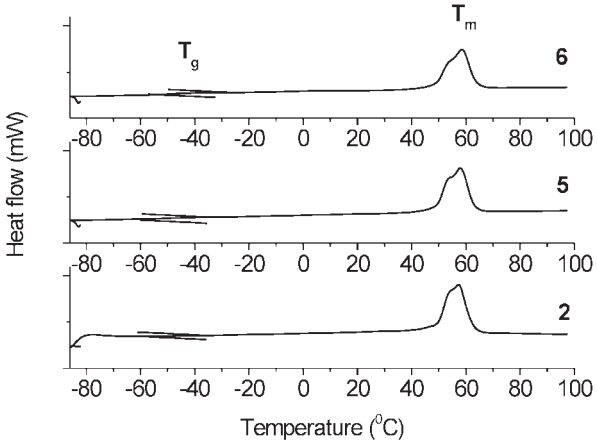

Figure 4. T_m characterization (DSC) of the second heating runs of polymers **2**, **5**, and **6**.

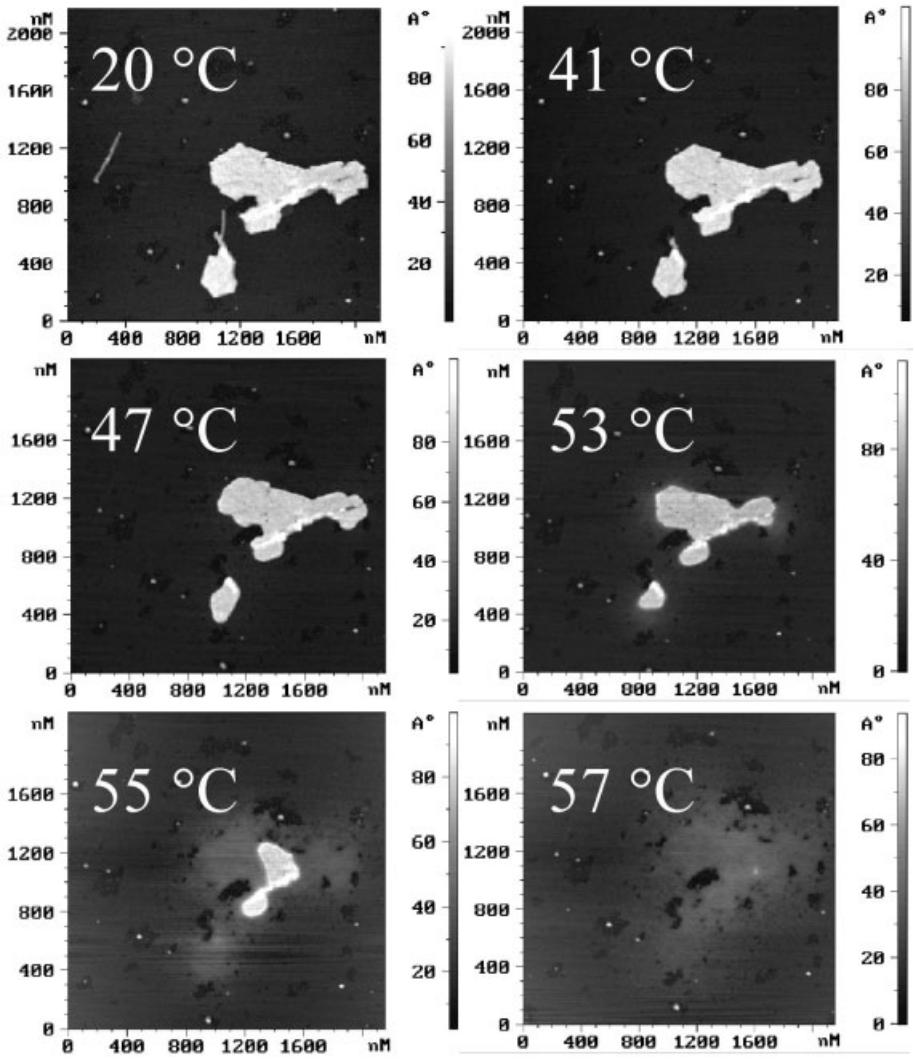

Figure 5. AFM height images of single crystals of **6** (recorded in the tapping mode). Increasing the temperature resulted in a melting process, which is depicted for 20, 41, 47, 53, 55, and 57 °C (molten crystals).

tion at 370 nm revealed an unstructured band with a maximum at 570 nm for **5** (Fig. 7). For **6**, an emission band with a maximum at 535 nm and a shoulder with a maximum at 570 nm (Fig. 7) were observed. The emission spectra [excitation wavelength (λ_{ex}) = 370 nm] of the polymer films of **5** and **6** were less pronounced, and both films emitted yellow light [**5**, maximum emission wavelength ($\lambda_{max,em}$) = 542 nm; **6**, $\lambda_{max,em}$ = 550 nm]. Excitation of the solutions of **5** and **6** with a UV lamp (λ_{ex} = 365 nm) allowed visualizing orange- (**5**) and greenish-yellow- (**6**) light emissions of the respective dichloromethane solutions and a yellow emission of a film of **6** (Fig. 8). Tables 2 and 3 summarize the optical properties of both polymers. The polymers showed favorable wet-processing features because of the film-forming nature of the PCL tail. Spin coating from a dichloromethane/acetonitrile (1/1 v/v) solvent mixture produced films without the appearance of crystals. Further improvement of such films could be obtained by annealing. The film quality obtained by inkjet printing is currently under investigation, as well as the performance of these polymers as light-emitting devices.

The redox properties of the macroligand complexes were determined by cyclic voltammetry (Fig. 9). The oxidation potentials agreed with literature data.[2,45] Only one active species was formed throughout the chelation reaction. An overview of the photophysical and electrochemi-

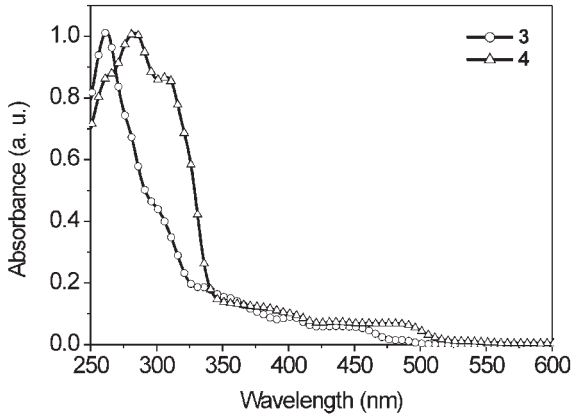

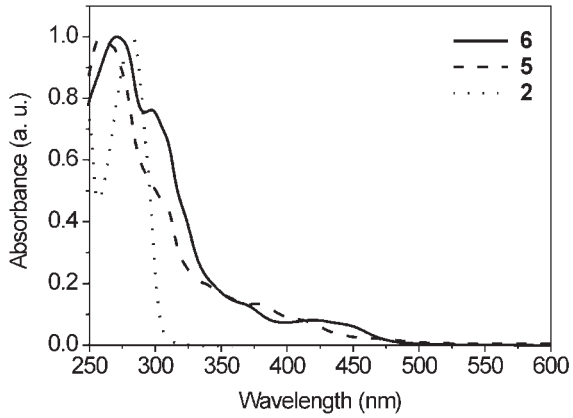

Figure 6. Absorption spectra of precursor complexes **3** and **4** and absorption spectra of polymers **5** and **6**. All spectra were recorded in CH_2Cl_2.

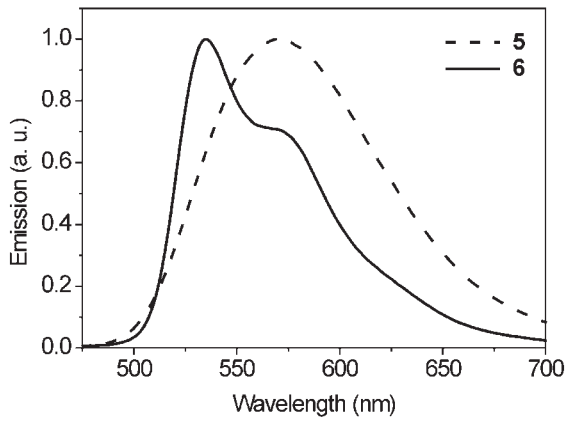

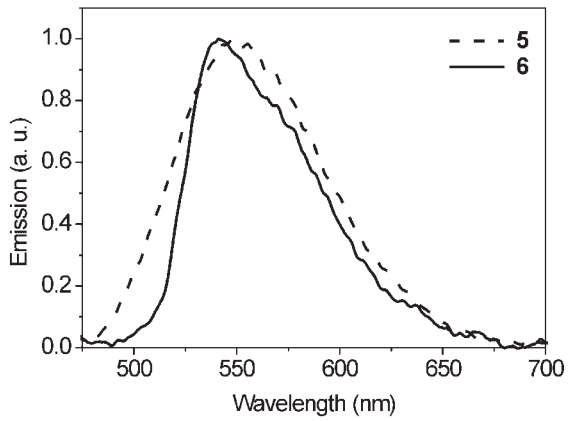

Figure 7. Emission properties of polymers **5** and **6** in CH_2Cl_2 solutions (top) and emission properties of films of polymers **5** and **6** (bottom).

cal properties of macroligand complexes **5** and **6** is given in Table 3.

CONCLUSIONS

We have described the synthesis of a bipyridine macroligand via a hydroxy-functionalized bpy ligand. The ROP of ϵ-caprolactone with hydroxy-functionalized bpy as the initiator was performed in a controlled fashion. The coordination of iridium(III) precursor complexes allowed us to prepare functional materials with valuable properties and potential for applications in various areas, such as device technology, biochemistry, and

Table 2. UV Characterization of Complexes **3** and **4** as well as **5** and **6** in CH_2Cl_2

	λ [nm; ϵ_{max} (L mol^{-1} cm^{-1})]
2	282 (9.9×10^3), 242 (7.6×10^3)
3	263 (6.5×10^4), 300 (2.8×10^4), 370 (7.4×10^3), 440 (3.8×10^3)
4	263 (6.5×10^4), 283 (7.5×10^4), 310 (6.4×10^4), 370 (9.4×10^3), 440 (5.4×10^3), 475 (5.0×10^3)
5	260 (1.7×10^5), 305 (7.9×10^4), 370 (2.2×10^4), 420 (1.1×10^4)
6	270 (1.5×10^5), 297 (1.2×10^5), 370 (2.1×10^4), 430 (1.2×10^4)

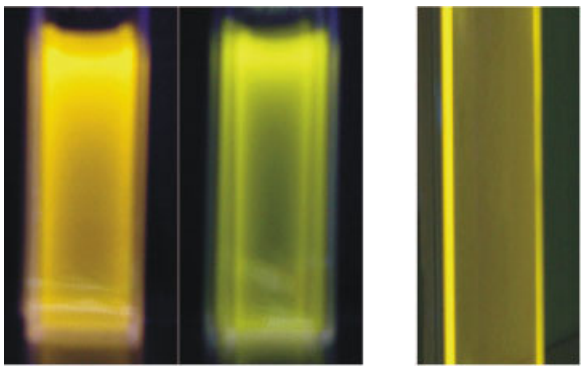

Figure 8. Representation of the different emission colors of CH_2Cl_2 solutions of polymeric complexes **5** (orange) and **6** (greenish-yellow). A film of **6** on a glass substrate (in a 1/1 v/v CH_2Cl_2/acetonitrile solution; spin-coated at 2000 rpm) is also displayed to visualize the yellow emission color.

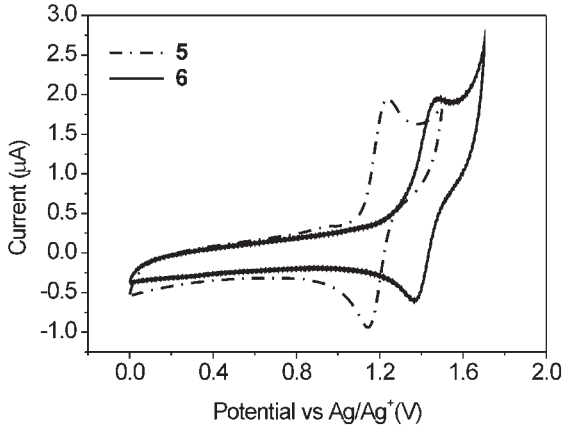

Figure 9. Cyclovoltammetry results of macroligand complexes **5** and **6**. All spectra were recorded in CH_2Cl_2 (freshly distilled from CaH_2) containing 0.1 M *n*-Bu_4PF_6 versus a Ag/Ag^+ reference electrode.

biomedicine. Characterization by NMR, IR, GPC, and MALDI-TOF MS proved the full complexation of the macroligand with the respective metal precursors. DSC was used to study the thermal behavior of the polymers. The melting process of single crystals of a PCL polymer was visualized by AFM. The metal-containing polymers displayed favorable photophysical and electrochemical properties, as well as good processing features, because of the film-forming properties of the PCL backbone. These novel complexes combined the features of a light-emitting complex and a polymer. This concept might be useful for preparing light-emitting devices by convenient and cost-effective wet-processing technologies such as spin coating and inkjet printing. In this way, the quick degradation of the emitters at the electrodes can be additionally suppressed. Moreover, aldehyde functionalities at the cyclometallating ligands provoked a significant change in the emission color in solution, giving rise to a new class of emissive polymers.

Table 3. Electrochemical and Optical Features of **5** and **6**

Compound	Oxidation Potential vs Fc/Fc^+ (eV)	$\lambda_{max,em}$ (nm)	Emission Color (λ_{ex} = 365 nm)
5 (solution)	1.23 (0.25)	570	Orange
6 (solution)	1.46 (0.26)	535	Greenish-yellow
5 (film)	—	542	Yellow
6 (film)	—	550	Yellow

This work forms part of the research program of Dutch Polymer Institute projects 291, 324, and 326. In addition, the authors thank the Fonds der Chemischen Industrie and Nederlandse Organisatie voor Wetenschappelijk Onderzoek (NWO) for their financial support. Rene Janssen and Martijn Wienk (Functional Molecules and Molecular Materials, Eindhoven University of Technology) are kindly acknowledged for granting access to the cyclovoltammetric and optical instrumentation. The authors also thank Michael A. R. Meier for performing the matrix-assisted laser desorption/ionization time- of-flight mass spectrometry measurements.

REFERENCES AND NOTES

1. Lo, K. K.-W.; Ng, D. C.-M.; Chung, C.-K. Organometallics 2001, 20, 4999.
2. Lo, K. K.-W.; Chung, C.-K.; Zhu, N. Chem—Eur J 2003, 9, 475.
3. Lo, K. K.-W.; Chung, C.-K.; Lee, T. K.-M.; Lui, L.-H.; Tsang, K. H.-K.; Zhu, N. Inorg Chem 2003, 42, 6886.
4. Lo, K. K.-W.; Chung, C.-K.; Ng, D. C.-M.; Zhu, N. New J Chem 2002, 26, 81.
5. Velonia, K.; Thordarson, P.; Andres, P. R.; Schubert, U. S.; Rowan, A. E.; Nolte, R. J. M. Polym Prepr 2003, 44, 648.
6. Staffilani, M.; Hoess, E.; Giesen, U.; Schneider, E.; Hartl, F.; Josel, H.-P.; De Cola, L. Inorg Chem 2003, 42, 7789.

7. Berggren, K.; Steinberg, T. H.; Lauber, W. M.; Carroll, J. A.; Lopez, M. F.; Chernokalskaya, E.; Zieske, L.; Diwu, Z.; Haugland, R. P.; Patton, W. F. Anal Biochem 1999, 276, 129.
8. Namba, Y.; Usami, M.; Suzuki, O. Anal Sci 1999, 15, 1087.
9. Duerkop, A.; Lehmann, F.; Wolfbeis, O. S. Anal Bioanal Chem 2002, 372, 688.
10. Dixon, I. M.; Collin, J.-P.; Sauvage, J.-P.; Flamigni, L.; Encinas, S.; Bargelletti, F. Chem Soc Rev 2000, 29, 385.
11. Lo, S.-C.; Namdas, E. B.; Burn, P. L.; Samuel, I. D. W. Macromolecules 2003, 36, 9721.
12. Beeby, A.; Bettington, S.; Samuel, I. D. W.; Wang, Z. J Mater Chem 2003, 13, 80.
13. Kalyuzhny, G.; Buda, M.; McNeill, J.; Barbara, P.; Bard, A. J. J Am Chem Soc 2003, 125, 6272.
14. Buda, M.; Kalyuzhny, G.; Bard, A. J. J Am Chem Soc 2002, 124, 6090.
15. Handy, E. S.; Pal, A. J.; Rubner, M. F. J Am Chem Soc 1999, 121, 3525.
16. Rudman, H.; Shimada, S.; Rubner, M. F. J Appl Phys 2003, 94, 115.
17. Rudmann, H.; Shimada, S.; Rubner, M. F. J Am Chem Soc 2002, 124, 4918.
18. Rudmann, H.; Rubner, M. F. J Appl Phys 2001, 90, 4338.
19. Slinker, J.; Bernards, D.; Houston, P. L.; Abruna, H. D.; Bernhard, S.; Malliaras, G. G. Chem Commun 2003, 19, 2392.
20. Lee, K. W.; Slinker, J. D.; Gorodetsky, A. A.; Flores-Torres, S.; Abruna, H. D.; Houston, P. L.; Malliaras, G. G. Phys Chem Chem Phys 2003, 5, 2706.
21. Holder, E.; Meier, M. A. R.; Marin, V.; Schubert, U. S. J Polym Sci Part A: Polym Chem 2003, 41, 3954.
22. Slinker, J. D.; Gorodetsky, A. A.; Lowry, M. S.; Wang, J.; Parker, S.; Rohl, R.; Bernhard, S.; Malliaras, G. G. J Am Chem Soc 2004, 126, 2763.
23. Noh, Y.-Y.; Lee, C.-L.; Kim, J.-J. J Chem Phys 2003, 118, 2853.
24. Anthopoulos, T. D.; Markham, J. P. J.; Namdas, E. B.; Samuel, I. D. W.; Lo, S.-C.; Burn, P. L. Appl Phys Lett 2003, 82, 4824.
25. Zhu, W. G.; Ke, Y.; Wang, F.; Liu, C. Z.; Yuan, M.; Cao, Y. Synth Met 2003, 137, 1079.
26. Gong, X.; Ostrowski, J. C.; Bazan, G. C.; Moses, D.; Heeger, A. J.; Liu, M. S.; Jen, A. K.-Y. Adv Mater 2003, 15, 45.
27. Zhu, W.; Liu, C.; Su, L.; Yang, W.; Yuan, M.; Cao, Y. J Mater Chem 2003, 13, 50.
28. Newkome, G. R.; Patri, A. K.; Holder, E.; Schubert, U. S. Eur J Org Chem 2004, 235.
29. (a) Schubert, U. S.; Eschbaumer, C. Angew Chem Int Ed 2002, 41, 2892; (b) Schubert, U. S.; Eschbaumer, C. Angew Chem 2002, 114, 3016.
30. Balzani, V.; Juris, A.; Venturi, M. Chem Rev 1996, 96, 759.
31. De Gans, B.-J.; Duineveld, P. C.; Schubert, U. S. Adv Mater 2004, 16, 203.
32. De Gans, B.-J.; Schubert, U. S. Macromol Rapid Commun 2003, 24, 659.
33. De Gans, B.-J.; Kazancioglu, E.; Meyer, W.; Schubert, U. S. Macromol Rapid Commun 2004, 25, 292.
34. Yang, S. Y.; Rubner, M. F. J Am Chem Soc 2002, 124, 2100.
35. Deshayes, G.; Mercier, F. A. G.; Degee, P.; Verbruggen, I.; Biesemans, M.; Willem, R.; Dubois, P. Chem—Eur J 2003, 9, 4346.
36. Corbin, P. S.; Webb, M. P.; McAlvin, J. E.; Fraser, C. L. Biomacromolecules 2001, 2, 223.
37. Marin, V.; Holder, E.; Schubert, U. S. J Polym Sci Part A: Polym Chem 2004, 42, 374.
38. Sprouse, S.; King, K. A.; Spellane, P. J.; Watts, R. J. J Am Chem Soc 1984, 106, 6647.
39. Neve, F.; Crispini, A.; Campagna, S.; Serroni, S. Inorg Chem 1999, 38, 2250.
40. Ciana, L. D.; Hamachi, I.; Meyer, T. J. J Org Chem 1989, 54, 1731.
41. Lo, K. K.-W.; Tsang, K. H.-K. Organometallics 2004, 23, 3062.
42. Meier, M. A. R.; Lohmeijer, B. G. G.; Schubert, U. S. Macromol Rapid Commun 2003, 24, 852.
43. Prokhorov, V. V.; Nitta, K.-H.; Terano, M. Macromol Chem Phys 2004, 205, 179.
44. Beekmans, L. G. M.; Vancso, G. J. Polymer 2000, 41, 8975.
45. Marin, V.; Holder, E.; Hoogenboom, R.; Schubert, U. S. J Polym Sci Part A: Polym Chem 2004, 42, 4153.